Ferrofluid-Controlled Liquid Metal IRS Unit Cell

Christopher Amendola, Ethan Chee, Ryan Taylor
Dept. of Electrical & Computer Engineering, Univ. Hawaii at Manoa
E-mail: camendol@hawaii.edu, ethanwc@hawaii.edu, jrtaylor@hawaii.edu

ABSTRACT: A functioning design for an intelligent reflective surface (IRS) was achieved between two states of a ferrofluid-actuated Galinstan slug. Reflection angle control from -13.3° to 90° was calculated to be feasible using the Generalized Snell's Law at a frequency of 8.3 GHz with an AABB unit cell configuration.

INTRODUCTION

IRS has the potential to revolutionize wireless communication systems. These surfaces are composed of an array of reconfigurable elements that can be programmed to manipulate and reflect incoming electromagnetic waves in specific ways. By controlling the phase, amplitude, and polarization of the reflected waves, IRS can enhance the signal quality and coverage in areas with poor wireless connectivity, reduce interference and power consumption. Current designs use a combination of complicated structures, diodes, and gravity to create different arrays.

An existing model from [1] uses two unit cell designs to create an array as shown in Fig. 1.

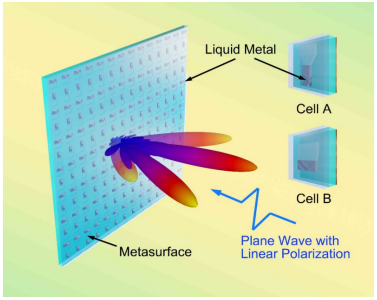

Fig. 1: The schematic of a liquid metal metasurface for flexible beam-steering.

The IRS was tested at 7.5 GHz and was able to achieve four different phases that are 90° apart from each other for any two adjacent states.

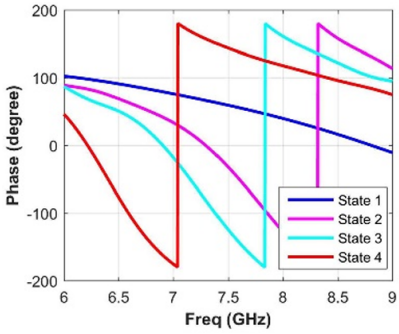

Fig. 2: The reflected phase responses of the proposed elements, with four different states.

However, this design relied on gravity-based actuation.

The proposed IRS unit cell design uses simple geometries similar to the design from Fig. 1 to achieve a 180° phase shift at different states with the force of gravity being negligent.

DESIGN & FABRICATION

The IRS unit cell is a symmetrical square shaped microfluidic channel design that uses Galinstan as the liquid metal and Fe_3O_4 based ferrofluid for the method of actuation. Each unit cell will have dimensions of 12 mm x 12 mm and the channel itself will be 10 mm x 10 mm, leaving a 1 mm gap between the channel and edge of the unit cell. Attaching an array of these unit cells will result in 2 mm gaps between each microfluidic channel. The channel will be half-filled with Galinstan, and the other half with ferrofluid, both with

dimensions of 10 mm x 5 mm. The unit cell will contain four electromagnets beneath the microfluidic channel layer, placed in the four corners 1 mm away from each edge of the channel. The electromagnets themselves will be 1 mm x 1 mm. The top view of the unit cell with the described dimensions is shown in Fig. 3.

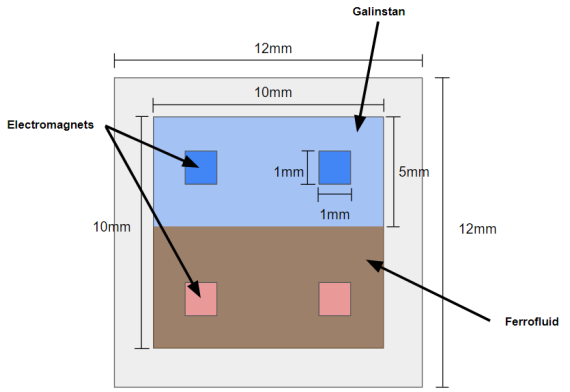

Fig. 3: Top view of IRS unit cell with view of the Galinstan, ferrofluid, and electromagnets.

The cross-sectional view of the unit cell can be viewed in Fig. 4. Starting from the bottom of the unit cell, there will be a 0.5 mm thick layer of copper to act as the ground plane. Above that is a 2 mm layer of RT/Duroid 5880 which will be the substrate for the unit cell. Within this same layer, there will be cutouts for the 1 mm^3 electromagnets that will perform the ferrofluidic actuation. To prevent any of the Galinstan or ferrofluid from making contact with the electromagnets, a 0.06 mm of kapton tape, or polyimide, will be used as a separation. Above this layer will be another layer of kapton tape with the 10 mm x 10 mm cutout for the Galinstan and ferrofluid. The final layer will be 0.06 mm of polystyrene.

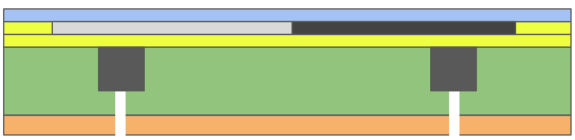

Fig. 4: Cross section of IRS unit cell.

To electrically control each of the four electromagnets within the RT/Duroid 5880 layer, there will be cutouts from the bottom of the copper ground plane up to the electromagnets as shown in Fig. 4. This will enable probes to be connected to the electromagnets where a current will be applied to create a magnetic field.

In addition to the material properties already available in Ansys HFSS, there were two materials not provided: Galinstan and Fe_3O_4 ferrofluid. Galinstan has a bulk conductivity of 3.46E+06 Siemens/m [2] and mass density of 6440 kg/m^3 [3]. An oil-based Fe_3O_4 ferrofluid has a resistivity of 10^3 Ω·cm [4], which equates to 0.1 Siemens/m, and a mass density of 1.2 g/mL [5], which equates to 1200 kg/m^3.

$$\sigma = \frac{1}{\rho} = \frac{1}{10^3 \Omega \cdot cm} = 0.1 \text{ Siemens/m}$$

$$\text{Mass Density} = 1.2\ g/mL = 1200\ kg/m^3$$

Since this IRS unit cell design has four electromagnets, there are a total of 2^4 = 16 possible configurations, but only four of those states will be tested. Those states are shown in Fig. 5.

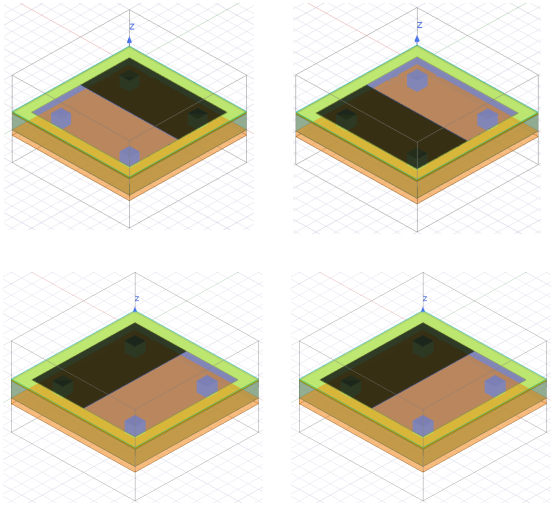

Fig. 5: State 1 (top left), State 2 (top right), State 3 (bottom left), State 4 (bottom right)

This microfluidic channel design was expected to produce identical results between states 1 and 2, and between states 3 and 4. This is because the geometry of the Galinstan does not physically change in those two states, but rather they are simply shifted which should not change the magnitude and phase plots. However, there should be a magnitude and phase difference between state 1 and 3 as the geometries are changed: the Galinstan slug has a 90° rotation difference compared to state 1. The ideal results for this design were to achieve a 180° phase shift between states 1 and 3 at a given frequency, as well as having an S_{11} magnitude of nearly 0 dB for both states at that same frequency. S_{11} defines the reflection coefficient of the unit cell and a value of 0 dB indicates that the reflected signal is the same magnitude as the incident signal. As the S_{11} magnitude in units of dB decreases below 0 dB, that will show loss which was not ideal. An acceptable range for this value would be between 0 dB and -1 dB.

SIMULATIONS

The unit cell was simulated on Ansys HFSS using the layer dimensions and materials described in the Design & Fabrication section. To insert the electromagnets into the RT/Duroid 5880 layer in the model, the Subtract tool was used. The same method was applied to create the cutout within the polyimide layer where the Galinstan and ferrofluid reside. In addition, an air box was added to enclose the entire unit cell. The HFSS model is shown in Fig. 5.

The method of excitation was the use of Floquet Ports to simulate an array of unit cells. To accomplish this, two primary and secondary boundaries were applied to the air box as shown in Fig. 6.

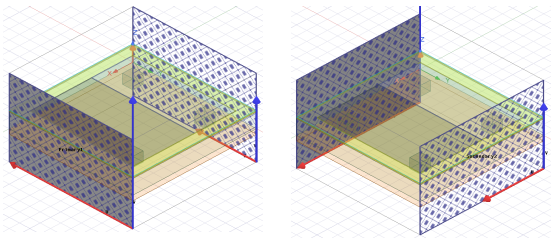

Fig. 6: Primary and secondary boundaries for the Floquet Port excitation.

Finally, the Floquet Port was applied to the top of the air box as shown in Fig. 7.

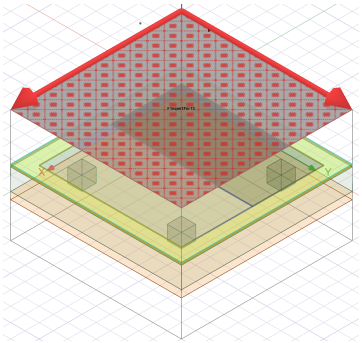

Fig. 7: Floquet Port excitation applied to the top plane of the air box.

The simulation was set to do a frequency sweep from 4 GHz to 10 GHz at a step size of 100 MHz. Both the S_{11} magnitude, in dB, and phase, in degrees, was plotted for both state 1 and state 3 of the unit cell. The S_{11} magnitude plot is shown in Fig. 8. The S_{11} phase plot is shown in Fig. 9. State 1 of the unit cell is shown in red and state 3 is shown in blue.

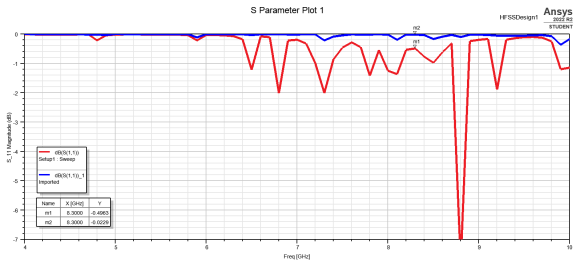

Fig. 8: S_{11} magnitude vs. frequency for states 1 and 3.

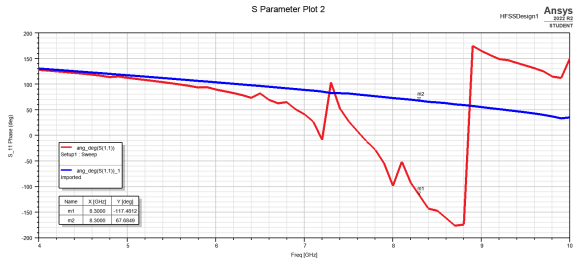

Fig. 9: S_{11} phase vs. frequency for states 1 and 3.

DISCUSSION

From the phase plot in Fig. 9, the 180° phase shift was achieved at a frequency of around 8.3 GHz. State 1 had a phase of -117.5° while state 3 had a phase of 67.7°, resulting in a phase shift of 185.2°. To verify if there was minimal loss at 8.3 GHz, the magnitude plot in Fig. 8 was analyzed. State 1 had a magnitude of -0.5 dB while state 3 had a magnitude of -0.02 dB. Both of these states had an S_{11} magnitude close to 0 dB, indicating that there was minimal loss in the reflected signal. Based on these results, it can be concluded that this IRS unit cell design can successfully steer an incident signal at a frequency of around 8.3 GHz with minimal loss.

Using this data, the Generalized Snell's Law (Eq. 1) was applied to calculate the angle of reflectance (Eq. 2) of a signal, given its angle of incidence.

$$sin\theta_r - sin\theta_i = \frac{\lambda_0}{2\pi}\frac{d\phi}{dx} \qquad (1)$$

$$\theta_r = arcsin\left(\frac{\lambda_0}{2\pi}\frac{d\phi}{dx} + sin\theta_i\right) \qquad (2)$$

The wavelength was calculated using the operating frequency of 8.3 GHz. This results in a wavelength of 36.14 mm.

$$\lambda_0 = \frac{c}{f} = \frac{3 \times 10^8\ m/s}{8.3 \times 10^9\ Hz} = 0.03614\ m$$

Two configurations of the state 1 and state 3 unit cells were tested with the Generalized Snell's Law. The first configuration was to have a 1x2 array where the first unit cell is state 1 and the second unit cell is state 3 as shown in Fig. 10. This will be noted as the 1-3 configuration.

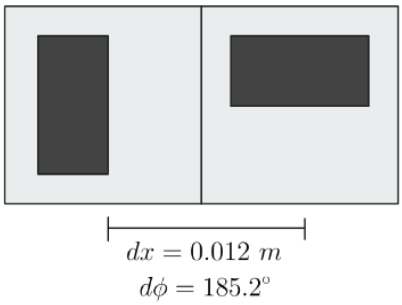

Fig. 10: 1-3 unit cell configuration on a 1x2 array.

The value of dx was determined from the distance between the center of each unit cell, which was 12 mm. Likewise, $d\phi$ was determined from the phase difference between each unit cell, which was 185.2°.

Using these calculated values, the angle of reflection θ_r was plotted against the angle of incidence θ_i using Eq. 2. The resulting graph is shown in Fig. 11.

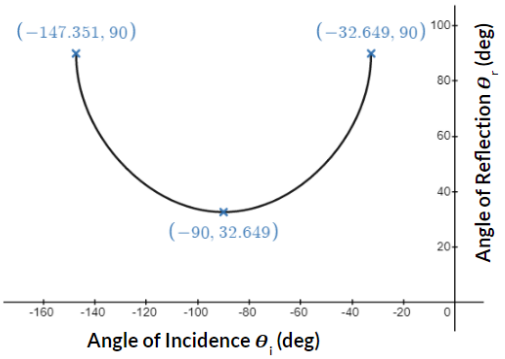

Fig. 11: Angle of reflection θ_r vs. angle of incidence θ_i for the 1-3 unit cell configuration.

This graph shows that the 1-3 configuration of this unit cell was capable of reflecting an incident signal from 32.65° to

90°, normal to the surface of the unit cell. For example, an incident signal at an angle of 38° would result in a reflected signal at an angle of 67.5° which can be visualized in Fig. 12.

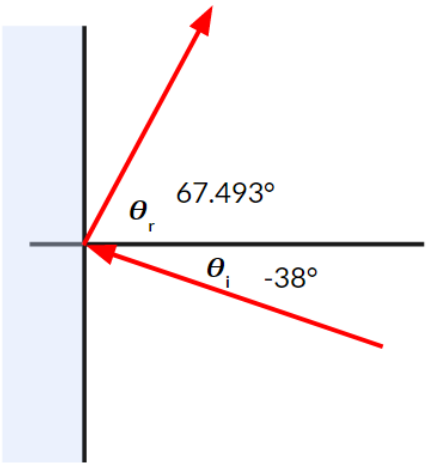

Fig. 12: Diagram of reflected signal with an incident angle of 38° and reflected angle of 67.493° from the normal.

The disadvantage of this configuration is that the generalized Snell's Law equation was not able to determine the angle of reflection for angles between 0° and 32.65°. To solve this issue, the 1-1-3-3 configuration was tested where four unit cells were combined into a 1x4 array. The two leftmost unit cells were in state 1 while the other two were in state 3, as shown in Fig. 13.

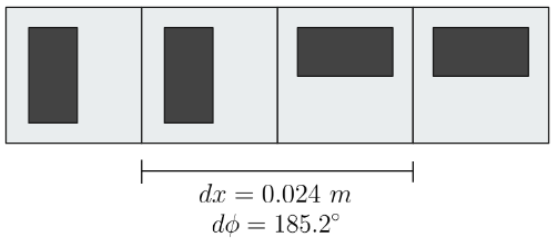

Fig. 13: 1-1-3-3 unit cell configuration on a 1x4 array.

The value of *dx* was determined from the distance between the center of the different unit cells, which was 24 mm. The value of *dϕ* remained the same value of 185.2° as the phase difference between state 1 and state 3 did not change in this configuration.

Using these calculated values, the angle of reflection θ_r was plotted against the angle of incidence θ_i using Eq. 2. The resulting graph is shown in Fig. 14.

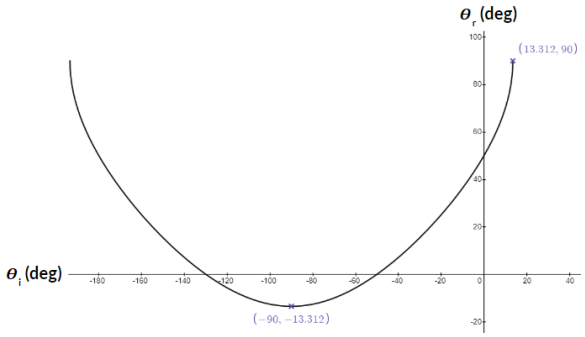

Fig. 14: Angle of reflection θ_r vs. angle of incidence θ_i for the 1-1-3-3 unit cell configuration.

This graph shows that the 1-1-3-3 configuration of this unit cell was capable of reflecting an incident signal from -13.3° to 90°, normal to the surface of the unit cell. Having this configuration of unit cells will successfully enable the IRS to reflect and steer any signals at 8.3 GHz from 0° to 90°, normal to the surface.

CONCLUSION

This design project demonstrates an effective design for an intelligent reflective surface (IRS) utilizing ferrofluid actuation to manipulate a Galinstan slug. Through simulations in HFSS and the application of the generalized Snell's law equation, the IRS exhibited the ability to control reflection angles from -13.3 degrees to 90 degrees for an 8.3 GHz signal with only slight loss of amplitude for the 1-1-3-3 configuration.

Future work that would further optimize the design and enhance our understanding of its capabilities could focus on simulating all possible configurations of the electromagnets that control the shape of the Galinstan, calculating the angles of

reflection for more configuration patterns, and employing the three-dimensional Snell's law equation to analyze the design's performance in both the x and y directions.

REFERENCES

[1] Chen, L., Ruan, Y., Cui, H. Y. (2019). Liquid Metal Metasurface for flexible beam-steering. Optics Express, 27(16), 23282. https://doi.org/10.1364/oe.27.023282

[2] Anwar, M.S., Ehlers, F. and Bangert, A. (2022), Experimental analysis of liquid metal galinstan for electronics actuation. Electron. Lett., 58: 617-619. https://doi.org/10.1049/ell2.12541

[3] "Galistan density melting point thermal conductivity." Material Properties. https://material-properties.org/galistan-density-melting-point-thermal-conductivity/ (accessed May 7, 2023).

[4] Electrically conductive ferrofluid compositions and method of preparing and using same, by K. Raj, et al. (1986, Aug. 5, 1986). Patent 4604229 [Online]. Available: https://patents.google.com/patent/US4604229A/en

[5] American Elements. "Ferrofluid." American Elements. https://www.americanelements.com/ferrofluid (accessed Apr. 26, 2023).